CHEMISTRY OF MATERIALS
Article

Chem. Mater. **2010,** *22,* 3277–3282 3277
DOI:10.1021/cm100603r

A General Approach to Noble Metal−Metal Oxide Dumbbell Nanoparticles and Their Catalytic Application for CO Oxidation

Chao Wang,*[,†,§] Hongfeng Yin,[‡] Sheng Dai,[‡] and Shouheng Sun*[,†]

[†]*Department of Chemistry, Brown University, 324 Brook Street, Providence, Rhode Island 02912, and* [‡]*Chemical Sciences Division, Oak Ridge National Laboratory, Oak Ridge, Tennessee 37831.* [§]*Current address: Materials Science Division, Argonne National Laboratory, 9700 S. Cass Ave., Argonne, IL 60439.*

Received February 26, 2010. Revised Manuscript Received April 7, 2010

Heterogeneous dumbbell-like nanoparticles represent an important type of composite nanomaterial that has attracted growing interest. Here we report a general approach to noble metal−metal oxide dumbbell nanoparticles based on seed-mediated growth. Metal oxides are grown over the presynthesized noble metal seeds by thermal decomposition of metal carbonyl followed by oxidation in air. The as-synthesized dumbbell nanoparticles have intrinsic epitaxial linkage between the metal and the oxide, providing enhanced heterojunction interactions. Moreover, the properties of one component are readily modified by the other in these nanoparticles, as demonstrated by the enhanced catalytic activity toward CO oxidation of such dumbbell nanoparticles in comparison with their counterparts prepared by conversional methods. The heterojunction effects provided in such nanostructures thus offer another degree of freedom for tailoring material properties. The developed synthetic strategy could also be generalized to other systems and thus represent a general approach to heterogeneous nanomaterials for various functional applications.

Introduction

Heterogeneous nanoparticles (NPs) containing two or more different functional units in epitaxial conjugation are of interest because of their unique electronic,[1] magnetic,[2] optical,[1a,3] and catalytic[4] properties. Such features mostly result from the nanoscale junction effects presented in the structure. It is known that for a heterojunction between a metal and metal oxide, the material properties at both sides close to the interface are modified from those in the bulk. This could be caused by many factors, including surface reconstruction around the junction,[5] lattice mismatch-induced crystal strain,[6] and electron interaction/transfer across the interface.[1a,2c,7] Nonetheless, tailoring material properties via heterogeneous conjugation to a large extent relies on the epitaxial linkage between the two different types of materials.

The importance of such composite NPs is further evidenced by the current intensive research for their applications in a variety of aspects. For example, the interaction between a semiconductor and metal in nanostructures has been utilized to study charge transfer for photovoltaics.[8] Nanoscale contact of Au NPs with a metal oxide surface makes the "inert" Au highly active in catalyzing CO oxidation.[9] Heterogeneous NPs containing optically responsive metal and magnetic NPs have been applied as multifunctional bioprobes for biomedical detection and imaging.[10] Understanding the interparticle interactions at the nanoscale level has become crucial in

*To whom correspondence should be addressed. E-mail: chaowang@anl.gov or ssun@brown.edu.

(1) (a) Yu, H.; Chen, M.; Rice, P. M.; Wang, S. X.; White, R. L.; Sun, S. H. *Nano Lett*. **2005**, *5*, 379–382. (b) Costi, R.; Cohen, G.; Salant, A.; Rabani, E.; Banin, U. *Nano Lett*. **2009**, *9*, 2031–2039.
(2) (a) Figuerola, A.; Fiore, A.; Di Corato, R.; Falqui, A.; Giannini, C.; Micotti, E.; Lascialfari, A.; Corti, M.; Cingolani, R.; Pellegrino, T.; Cozzoli, P. D.; Manna, L. *J. Am. Chem. Soc*. **2008**, *130*, 1477–1487. (b) Teranishi, T.; Wachi, A.; Kanehara, M.; Shoji, T.; Sakuma, N.; Nakaya, M. *J. Am. Chem. Soc*. **2008**, *130*, 4210–4211. (c) Frey, N. A.; Phan, M. H.; Srikanth, H.; Srinath, S.; Wang, C.; Sun, S. *J. Appl. Phys*. **2009**No. 07B502.
(3) (a) Gu, H. W.; Zheng, R. K.; Zhang, X. X.; Xu, B. *J. Am. Chem. Soc*. **2004**, *126*, 5664–5665. (b) Jiang, J.; Gu, H. W.; Shao, H. L.; Devlin, E.; Papaefthymiou, G. C.; Ying, J. Y. *Adv. Mater*. **2008**, *20*, 4403–4407. (c) Kwon, K. W.; Shim, M. *J. Am. Chem. Soc*. **2005**, *127*, 10269–10275. (d) Wei, Y. H.; Klajn, R.; Pinchuk, A. O.; Grzybowski, B. A. *Small* **2008**, *4*, 1635–1639.
(4) (a) Elmalem, E.; Saunders, A. E.; Costi, R.; Salant, A.; Banin, U. *Adv. Mater*. **2008**, *20*, 4312–4317. (b) Wang, C.; Daimon, H.; Sun, S. H. *Nano Lett*. **2009**, *9*, 1493–1496.
(5) (a) Weiss, W.; Ritter, M. *Phys. Rev. B* **1999**, *59*, 5201–5213. (b) El-Deab, M. S.; Ohsaka, T. *Angew. Chem., Int. Ed*. **2006**, *45*, 5963–5966.
(6) (a) Gilbert, B.; Huang, F.; Zhang, H. Z.; Waychunas, G. A.; Banfield, J. F. *Science* **2004**, *305*, 651–654. (b) Huang, W. J.; Sun, R.; Tao, J.; Menard, L. D.; Nuzzo, R. G.; Zuo, J. M. *Nat. Mater*. **2008**, *7*, 308–313. (c) Zhou, X. X.; Wang, Y. B.; Gu, Q.; Li, W. F. *Aquaculture* **2009**, *291*, 78–81.
(7) Liu, Z. P.; Gong, X. Q.; Kohanoff, J.; Sanchez, C.; Hu, P. *Phys. Rev. Lett*. **2003**, 91.
(8) (a) Adams, D. M.; Brus, L.; Chidsey, C. E. D.; Creager, S.; Creutz, C.; Kagan, C. R.; Kamat, P. V.; Lieberman, M.; Lindsay, S.; Marcus, R. A.; Metzger, R. M.; Michel-Beyerle, M. E.; Miller, J. R.; Newton, M. D.; Rolison, D. R.; Sankey, O.; Schanze, K. S.; Yardley, J.; Zhu, X. Y. *J. Phys. Chem. B* **2003**, *107*, 6668–6697. (b) Pompa, P. P. *Nat. Nanotechnol*. **2006**, *1*, 126–130. (c) Jin, Y.; Gao, X. *Nat. Nanotechnol*. **2009**, *4*, 571–576.
(9) Haruta, M.; Kobayashi, T.; Sano, H.; Yamada, N. *Chem. Lett*. **1987**, 405–408.
(10) (a) Choi, J. S.; Jun, Y. W.; Yeon, S. I.; Kim, H. C.; Shin, J. S.; Cheon, J. *J. Am. Chem. Soc*. **2006**, *128*, 15982–15983. (b) Xu, C.; Xie, J.; Ho, D.; Wang, C.; Kohler, N.; Walsh, E. G.; Morgan, J. R.; Chin, Y. E.; Sun, S. *Angew. Chem., Int. Ed*. **2008**, *47*, 173–176.

Published on Web 04/26/2010

Scheme 1. Seed-Mediated Growth for Noble Metal−Metal Oxide NPs

designing advanced composite nanomaterials for property optimization today.[11]

Here we report a general approach to noble metal−metal oxide dumbbell NPs via organic solvothermal synthesis. Through a seed-mediated growth method (Scheme 1), we have been able to synthesize noble metal−metal oxide dumbbell NPs with the metal oxide epitaxially grown over the noble metal particles. The approach has been demonstrated to be robust because of the success in preparing NPs of diversified materials, with noble metals of Au, Ag, Pt, or AuAg alloy and oxides of iron or cobalt. Catalytic study has revealed that, for example, Au−Fe_3O_4 and Pt−Fe_3O_4 NPs exhibit enhanced catalytic activity toward CO oxidation compared to their conventional counterparts.

Experimental Section

Nanoparticle Synthesis. *Au NPs.* A solution of tetralin (10 mL), oleylamine (10 mL), and $HAuCl_4 \cdot 3H_2O$ (0.1 g) was prepared in air at 20 °C and magnetically stirred under a nitrogen flow; 0.5 mmol of a *tert*-butylamine−borane complex was dissolved in tetralin (1 mL) and oleylamine (1 mL) and injected into the precursor solution. The reaction was initiated instantaneously, and the color of the solution changed to deep purple within 5 s. The mixture was allowed to be aged at 20 °C for 1 h before acetone (60 mL) was added to precipitate the Au NPs. The Au NPs were collected by centrifugation, washed with acetone, and redispersed in hexane.

Ag NPs. $AgNO_3$ (1 mmol) was dissolved in 20 mL of oleylamine to form a solution. The solution was slowly heated to 120 °C under a nitrogen flow. NP growth was conducted at this temperature for 1 h. After the mixture had cooled to room temperature, 30 mL of ethanol was added to the solution, and the NPs were separated with a centrifuge. The precipitate was dispersed in hexane. After being washed three times using ethanol, the product was dispersed in 15 mL of hexane.

Pt NPs. For 3 nm Pt NPs, platinum actylacetonate [$Pt(acac)_2$, 0.1 g], 1-octadecene (ODE, 10 mL), oleic acid (1 mL), and oleylamine (1 mL) were mixed under N_2 and magnetic stirring. The mixture was then heated to ~65 °C to dissolve the Pt salt. The temperature was then increased to ~180 °C. A hexane solution of $Fe(CO)_5$ [0.1 mL, prepared by addition of 0.1 mL of $Fe(CO)_5$ in 1 mL of hexane under argon] was quickly injected into the hot solution. The solution was further heated to 200 °C and kept at this temperature for 1 h before it was cooled to room temperature; 40 mL of 2-propanol was added, and then the suspension was centrifuged to separate the NPs. The particles were washed with ethanol and then dispersed in 10 mL of hexane for further use; 5 and 7 nm Pt NPs were synthesized by similar procedures except that the $Fe(CO)_5$ solution was injected at 160 and 120 °C, respectively.

AuAg Alloy NPs. $AgNO_3$ (2 mmol) was dissolved in 20 mL of oleylamine. The solution was slowly heated to 100 °C under a nitrogen flow. A $HAuCl_4$ solution (0.2 mmol of $HAuCl_4$ in 5 mL of 1-octadecene with 1 mL of oleylamine) was injected into the hot solution. The solution temperature was then kept at 120 °C for 0.5 h before the mixture was cooled to room temperature. NPs obtained from this case have a $Au_{0.82}Ag_{0.18}$ composition [measured by energy-dispersive spectroscopy (EDX)]. By changing the precursor ratio and growth time, we can continuously tune the composition from Au-rich to Ag-rich. For example, with 2 mmol of $AgNO_3$ and 0.2 mmol of $HAuCl_4$, extending the growth time to 1 h (at 120 °C) led to $Au_{0.60}Ag_{0.40}$ NPs. Ag-rich NPs can be obtained by further increasing the amount of silver precursor. With 4 mmol of $AgNO_3$ and 0.2 mmol of $HAuCl_4$, growth for 1 h led to $Au_{0.52}Ag_{0.48}$ NPs while growth for 2 h gave $Au_{0.39}Ag_{0.61}$ NPs.

Pt−Fe_3O_4 Dumbbell NPs. For 3−10 nm Pt−Fe_3O_4 NPs, 1-octadecene (20 mL) and oleic acid (1 mL) were mixed and stirred. The mixture was degassed at 120 °C under a nitrogen flow for 30 min. Under a N_2 blanket, $Fe(CO)_5$ (0.14 mL, 1 mmol) was added. After 10 min, oleylamine (97%, Acros) (1 mL) was added and 3 nm Pt seeds (20 mg, dispersed in 2 mL of hexane) were injected into this hot solution. The resulting solution was heated to 300 °C and kept at this temperature for 20 min before it was cooled to room temperature via removal of the heating mantle; 60 mL of absolute ethanol was added to precipitate the product, followed by centrifugation. The precipitated NPs were dispersed into hexane, precipitated out by ethanol, and centrifuged. The process was repeated two times to purify the NPs. The final product was dispersed in 10 mL of hexane.

On the basis of the reaction conditions described above, 0.1 mL of $Fe(CO)_5$ led to the formation of 3−7 nm Pt−Fe_3O_4 NPs. With 20 mg of 5 nm Pt seeds, 0.14 mL of $Fe(CO)_5$ gave 5−17 nm Pt−Fe_3O_4 NPs and 0.1 mg of $Fe(CO)_5$ yielded 5−12 nm Pt−Fe_3O_4 NPs.

Au(Ag,AuAg)−Fe_3O_4 Dumbbell NPs. The recipe is similar to that described above for Pt−Fe_3O_4 NPs, except Au (Ag, Pd, or AuAg) NPs were added as seeds instead of Pt.

Au(Ag,Pt,AuAg)−CoO Dumbbell NPs. Diphenyl ether (20 mL) and oleic acid (1 mL) were mixed and degassed at 120 °C for 30 min; 0.5 mmol of $Co_2(CO)_8$ was added to this hot solution, followed by 1 mL of oleylamine after 5 min. Seeding NPs (11 mg) dispersed in 1 mL of hexane were quickly injected into this solution. The resulting solution was heated to 260 °C and kept in reflux for 30 min.

Characterizations. Samples for transmission electron microscopy (TEM) analysis were prepared by depositing one drop of a diluted NP dispersion in hexane on amorphous carbon-coated copper grids. Images were obtained with a Philips EM 420 instrument (120 kV). The high-resolution TEM (HRTEM) image was obtained on a JEOL 2010 TEM instrument (200 kV). X-ray diffraction (XRD) patterns were obtained on a Bruker AXS D8-Advance diffractometer with Cu Kα radiation (λ = 1.5418 Å). Quantitative elemental analyses were conducted on a LEO 1560 SEM instrument equipped with spatially resolved energy dispersive X-ray spectroscopy (EDX). Samples for EDX were prepared by depositing the NP dispersion on a silicon substrate, and solvent was allowed to evaporate under ambient conditions. UV−vis spectra were recorded on a PerkinElmer Lamda 35 spectrometer using quartz cuvettes.

Catalytic Study. Au−Fe_3O_4 or Pt−Fe_3O_4 NPs (1 mL) were dissolved in 20 mL of hexane and stirred for 10 min before

(11) Wang, C.; Xu, C. J.; Zeng, H.; Sun, S. H. *Adv. Mater.* **2009**, *21*, 3045–3052.

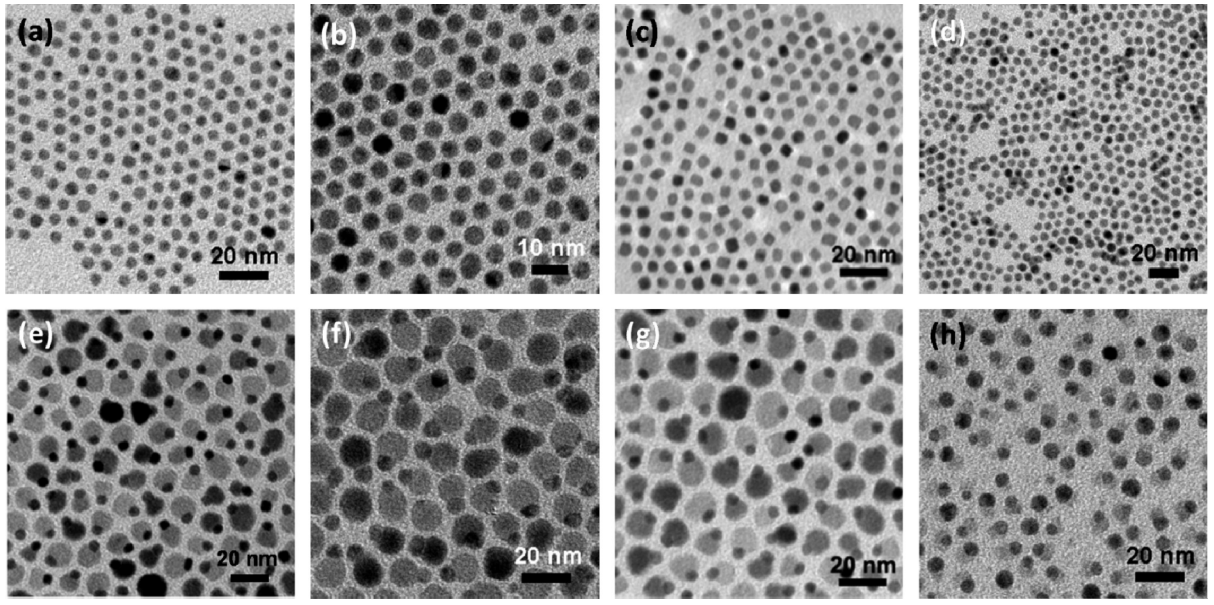

Figure 1. TEM images of (a) 5 nm Au, (b) 5 nm Ag, (c) 5 nm Pt, (d) 6 nm AuAg, (e) 5−12 nm Au−Fe_3O_4, (f) 5−12 nm Ag−Fe_3O_4, (g) 5−12 nm Pt−Fe_3O_4, and (h) 6−10 nm AuAg−Fe_3O_4 NPs.

0.160 g of SiO_2 (cabosil) was added. The suspension was stirred overnight to evaporate hexane. The resulting solid was washed with hexane and dried under vacuum. EDX showed that the contents of noble metal in the prepared catalysts were 1.67% for Au and 2.25% for Pt in weight. For CO oxidation, 50 mg of each catalyst was packed in a U-tube with quartz wool and calcined in an 8% O_2/He atmosphere at 300 °C for 1 h to remove organic residues and moisture (Fe_3O_4 was oxidized to Fe_2O_3 after the calcination). The catalyst was subsequently cooled to room temperature, and the gas stream was switched to 1% CO (balanced with air, <4 ppm H_2O) at a flow rate of 37 cm^3/min [corresponding to a space velocity of 41900 cm^3 h^{-1} (g of catalyst)$^{-1}$]. A portion of the product stream was extracted periodically with an automatic sampling valve at different reaction temperatures and analyzed with a dual-column gas chromatograph with a thermal conductivity detector. A commercial Au−Fe_2O_3 catalyst (World Gold Council, 5% Au in weight) treated via the same procedures was used in the control experiment.

Results and Discussion

To make dumbbell-like NPs, the key step is to prepare monodisperse seeding NPs with proper size and surface. Seed sizes of <10 nm would facilitate the control of epitaxial overgrowth since otherwise the large particles tend to precipitate in the seeded growth of noble metal−metal oxide NPs. The surface ligand used in the seed preparation is also important, which should be compatible with the subsequent growth conditions and not bond too strongly to the particle surface. For example, thiol can hinder the epitaxial overgrowth of metal oxides on noble metal NPs, producing composite NPs showing nearly independent material properties of each component.[12] With the proper seeding NPs, metal oxide was then overgrown via a seed-mediated approach by thermal decomposition of metal carbonyl followed by oxidation in air (Scheme 1).[1a]

We have employed organic solution synthesis with rather weak ligands to grow the noble metal seeds, i.e., oleylamine and oleic acid which are bonding to the noble metal surface not that strongly (the details of synthesis are presented in the Supporting Information). Figure 1 shows the TEM images of the noble metal−Fe_3O_4 NPs and the related noble metal seeds. Monodisperse 6 nm Au NPs were obtained via a quick reduction of Au precursor ($AuCl_4^-$) by a *tert*-butylamine−borane complex at 20 °C (Figure 1a).[13] The size of Au particles can be further tuned by the reaction temperature, with higher temperatures leading to smaller Au NPs (e.g., 2.4 nm Au NPs were obtained at 40 °C and 9.5 nm NPs at 2 °C);[13b] 5 nm Ag seeds were prepared by thermal reduction of $AgNO_3$ with oleylamine at 120 °C (Figure 1b), where oleylamine served as the solvent, the reducing agent, and the stabilizing surfactant. Injection of the $HAuCl_4$ precursor into the hot oleylamine solution of $AgNO_3$ before Ag nucleation started (~100 °C) gave AuAg alloy NPs (Figure 1c), with the alloy composition readily tuned by the ratio between Au and Ag precursors.[14] Pt seeds were synthesized by thermal reduction of $Pt(acac)_2$ by oleylamine in the presence of a trace amount of $Fe(CO)_5$. $Fe(CO)_5$ was used to control the Pt nucleation and to achieve Pt size control. Via addition of the $Fe(CO)_5$ solution at 160 °C, 5 nm Pt NPs were obtained (Figure 1d).[15] The seeds were thus mixed with $Fe(CO)_5$ in a nonpolar solvent (1-octadecene) at a mild temperature (~120 °C), where $Fe(CO)_5$ decomposition had not started while the seeding NPs were still

(12) (a) Gu, H. W.; Yang, Z. M.; Gao, J. H.; Chang, C. K.; Xu, B. *J. Am. Chem. Soc.* **2005**, *127*, 34–35. (b) Zhang, L.; Dou, Y. H.; Gu, H. C. *J. Colloid Interface Sci.* **2006**, *297*, 660–664.

(13) (a) Zheng, N.; Fan, J.; Stucky, G. D. *J. Am. Chem. Soc.* **2006**, *128*, 6550–6551. (b) Peng, S.; Lee, Y.; Wang, C.; Yin, H.; Dai, S.; Sun, S. *Nano Res.* **2008**, *1*, 229–234.

(14) Wang, C.; Yin, H. G.; Chan, R.; Peng, S.; Dai, S.; Sun, S. H. *Chem. Mater.* **2009**, *21*, 433–435.

(15) Wang, C.; Daimon, H.; Onodera, T.; Koda, T.; Sun, S. H. *Angew. Chem., Int. Ed.* **2008**, *47*, 3588–3591.

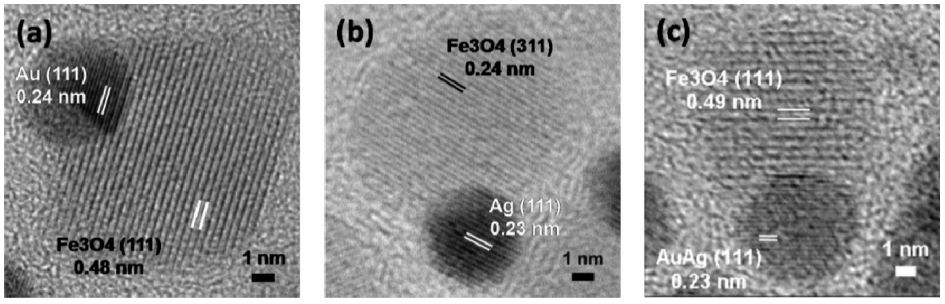

Figure 2. HRTEM images of (a) Au−Fe_3O_4, (b) Ag−Fe_3O_4, and (c) AuAg−Fe_3O_4 NPs.

stable (particularly for thermally unstable Au, Ag, and AuAg NPs), before the solution was heated to reflux for growing dumbbell NPs. Monodisperse 5−12 nm Au−Fe_3O_4 (Figure 1e), 5−12 nm Ag−Fe_3O_4 (Figure 1f), 5−12 nm Pt−Fe_3O_4 (Figure 1g), and 6−10 nm AuAg−Fe_3O_4 (Figure 1h) NPs were obtained with 20 mg of the noble metal seeds and 1 mmol of $Fe(CO)_5$.

Similar strategies have also been successfully applied for the synthesis of other noble metal−metal oxide NPs, like Pd−Fe_3O_4 (Figure S1 of the Supporting Information) and Au,Pt−CoO (Figure S2 of the Supporting Information). The Pd seeds prepared by the current recipe have a size of ∼1.5 nm. Metal oxide growth over such small seeds gives almost full encapsulation of the seed, leaving only a small fraction of the noble metal surface exposed (Figure S1c of the Supporting Information). The case of cobalt oxide overgrowth is somehow different from that of Fe_3O_4, as the decomposition of $Co_2(CO)_8$ under the conditions described here usually gives highly disordered Co nanocrystals and their follow-up oxidation in air forms CoO of very poor crystallinity (Figure S3 of the Supporting Information).[16] This nature of CoO reduced the controllability and leads to the irregular shape of the overgrown oxide NPs. Further annealing might be required to crystallize the cobalt oxide for potential applications.[16b,17]

HRTEM images reveal the epitaxial relationship between the noble metal and metal oxide in the composite NPs. Figure 2 shows the HRTEM images of Au, Ag, and AuAg−Fe_3O_4 NPs with lattice fringes. The interfringe distances were measured to be 0.23−0.24 nm for the noble metal particles, corresponding to the (111) plane of fcc Au or Ag. While (111) fringes were commonly observed for noble metal particles, the situation is more complicated for metal oxide NPs. The interfringe distance was measured to be 0.48−0.49 nm for the metal oxide particle in panels a and c of Figure 2, while 0.24 nm for the particle in Figure 2b, corresponding to (111) and (311) planes of inverse spinel structured magnetite, respectively. The epitaxial relationship between the noble metal and the metal oxide particles is thus evidenced by either the small mismatch between Fe_3O_4 (311) and Ag (111) [< 5% (Figure 2b)] or the interfringe distance of Fe_3O_4 (111) being 2 times that of Au or AuAg (111) (Figure 2a,c).

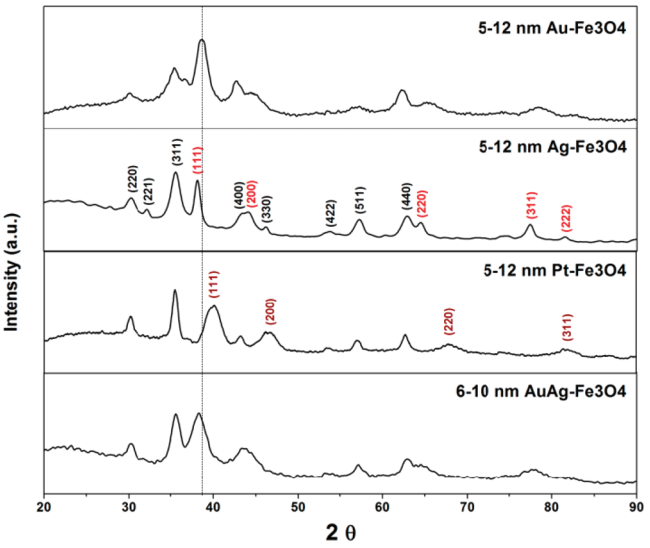

Figure 3. XRD patterns of the noble metal−metal oxide NPs. The red peak labels are for the fcc phase of the noble metals while the black labels for inverse spinel structured Fe_3O_4 (magnetite). The position of the Au (111) peak is indicated with a dashed line to guide the view.

The crystal structures of the noble metal−Fe_3O_4 NPs are further confirmed by XRD. Figure 3 shows the XRD patterns of the four types of composite NPs. All of them show two sets of peaks, corresponding to fcc Au, Ag, or AuAg alloy (marked in red) and magnetite (marked in black). It can also be seen that the peaks for Pt have a shift toward a higher angle than those for Au and Ag, with the (111) peak at 38.7° for Au, 38.0° for Ag, and 40.1° for Pt, consistent with the trend in lattice constants among these noble metals: Pt (3.92 Å) < Au (4.08 Å) < Ag (4.09 Å).

The epitaxial linkage between the metal and oxide in the composite NPs has a significant effect on the properties of individual particles. For example, Figure 4a shows the UV−vis spectra of Au−Fe_3O_4 NPs, where the surface plasmon resonance (SPR) peak is broadened and has a red shift (520 nm) compared with that of the Au seeds (515 nm). Similar changes were also observed for the other NPs (e.g., Figure 4b for AuAg−Fe_3O_4 NPs). While the SPR peak broadening can be caused by damping caused by the electronic coupling between metal and oxide, the red shift has been ascribed to electron transfer across the metal−oxide interface.[1a] Such interactions could modify the electronic structure of each component,[2c,4b] which can be utilized to tailor material properties for functional applications.

(16) (a) Sun, S. H.; Murray, C. B. *J. Appl. Phys.* **1999**, *85*, 4325–4330. (b) Wang, C.; Peng, S.; Lacroix, L. M.; Sun, S. H. *Nano Res.* **2009**, *2*, 380–385.
(17) Black, C. T.; Murray, C. B.; Sandstrom, R. L.; Sun, S. H. *Science* **2000**, *290*, 1131–1134.

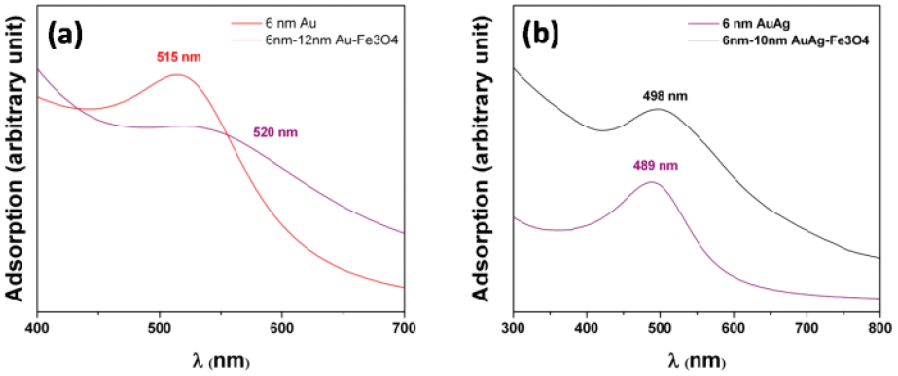

Figure 4. UV−vis spectra of (a) Au and Au−Fe_3O_4 and (b) AuAg and AuAg−Fe_3O_4 NPs.

Oxidation and removal of CO from the feeding gas is one of the key reactions in the contexts of both cleaning air and energy conversion. Conventionally, CO oxidation is catalyzed by Pt-based catalysts. This scheme works well at high temperatures, but the efficiency substantially decays when the temperature drops to near room temperature. Thanks to Haruta's pioneering work on the highly active Au−Fe_2O_3 catalyst for CO oxidation, recent efforts have been focused on heterogeneous noble metal−metal oxide composites, which are usually prepared by precipitation deposition,[18] coprecipitation,[19] ligand-assisted deposition,[20] ion exchange,[21] or colloidal deposition.[22] Among them, the colloidal deposition approach is particularly promising because of the recent advancement in solution-phase syntheses of various noble metal NPs with control of size, shape, and composition. In addition, sequentially synthesis and deposition of these NPs on supports avoid the constraint that the support surface properties have to be compatible with the deposition conditions of noble metal elements (e.g., isoelectric point). However, such a traditional colloidal deposition approach usually suffers from a lack of direct chemical noble metal−metal oxide interactions between the presynthesized noble metal NPs and the metal oxide matrix, while physically supported noble metal particles are inactive at low temperatures.[23] Furthermore, these catalytic systems have limited thermal stabilities, and the noble metal NPs often sinter under high-temperature reaction conditions, which causes a significant decrease in the level of catalytic performance of the catalyst.[18d,22a]

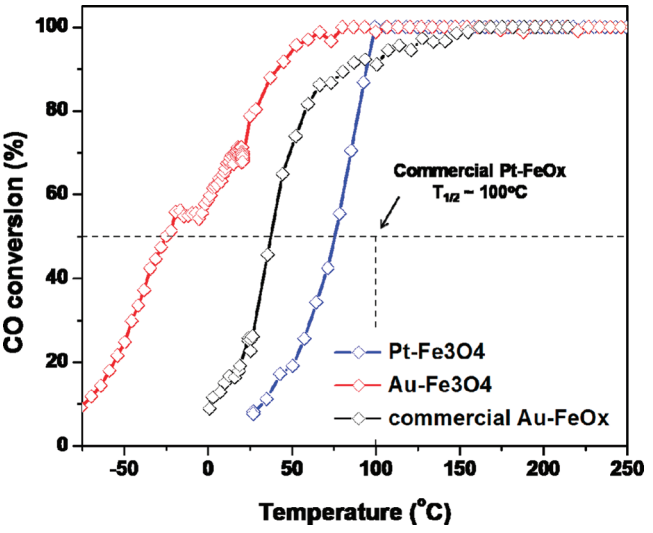

Figure 5. CO oxidation conversion light-off curves of Au−Fe_3O_4 and Pt−Fe_3O_4 NPs and commercial Au/Fe_2O_3 (World Gold Council) catalyst. The marked $T_{1/2}$ value of conventional Pt/Fe_2O_3 was adopted from ref 25. Note that isolated Au or Pt NPs are not active in the related temperature range.

The noble metal−metal oxide NPs prepared here offer an approach to overcoming the obstacles described above while preserving the advantages of the colloidal deposition method. Figure 5 shows the conversion light-off curves of Au− and Pt−Fe_3O_4 catalysts for CO oxidation. Au−Fe_3O_4 and Pt−Fe_3O_4 NPs were deposited on SiO_2 according to a previously reported method and calcinated at 300 °C in an oxygenated atmosphere, where no significant change in particle size and the noble metal−Fe_3O_4 heterojunctions were preserved after calcinations.[24] The results for Au/Fe_2O_3 (from World Gold Council, 5% Au in weight) and $T_{1/2}$ (the temperature at which CO conversion reaches 50%) of Pt/Fe_2O_3[25] catalysts prepared by the conventional method with the same treatment (annealed at 300 °C in an oxygenated atmosphere) are also presented for the sake of comparison. We find that both the Au− and Pt−Fe_3O_4 NPs are more active than their conventional counterparts. The Au−Fe_3O_4 NPs

(18) (a) Haruta, M. *Gold Bull.* (*London, U.K.*) **2004**, *37*, 27–36. (b) Zanella, R.; Giorgio, S.; Henry, C. R.; Louis, C. *J. Phys. Chem. B* **2002**, *106*, 7634–7642. (c) Kung, H. H.; Kung, M. C.; Costello, C. K. *J. Catal.* **2003**, *216*, 425–432. (d) Yan, W. F.; Mahurin, S. M.; Pan, Z. W.; Overbury, S. H.; Dai, S. *J. Am. Chem. Soc.* **2005**, *127*, 10480–10481. (e) Calla, J. T.; Bore, M. T.; Datye, A. K.; Davis, R. J. *J. Catal.* **2006**, *238*, 458–467.
(19) (a) Wang, A. Q.; Hsieh, Y.; Chen, Y. F.; Mou, C. Y. *J. Catal.* **2006**, *237*, 197–206. (b) Fu, Q.; Saltsburg, H.; Flytzani-Stephanopoulos, M. *Science* **2003**, *301*, 935–938.
(20) (a) Bore, M. T.; Pham, H. N.; Ward, T. L.; Datye, A. K. *Chem. Commun.* **2004**, 2620–2621. (b) Budroni, G.; Corma, A. *Angew. Chem., Int. Ed.* **2006**, *45*, 3328–3331. (c) Scott, R. W. J.; Sivadinarayana, C.; Wilson, O. M.; Yan, Z.; Goodman, D. W.; Crooks, R. M. *J. Am. Chem. Soc.* **2005**, *127*, 1380–1381.
(21) (a) Zanella, R.; Sandoval, A.; Santiago, P.; Basiuk, V. A.; Saniger, J. M. *J. Phys. Chem. B* **2006**, *110*, 8559–8565. (b) Zhu, H. G.; Liang, C. D.; Yan, W. F.; Overbury, S. H.; Dai, S. *J. Phys. Chem. B* **2006**, *110*, 10842–10848.
(22) (a) Comotti, M.; Li, W. C.; Spliethoff, B.; Schuth, F. *J. Am. Chem. Soc.* **2006**, *128*, 917–924. (b) Zheng, N. F.; Stucky, G. D. *J. Am. Chem. Soc.* **2006**, *128*, 14278–14280.
(23) Goodman, D. W. *Catal. Lett.* **2005**, *99*, 1–4.
(24) Yin, H. F.; Wang, C.; Zhu, H. G.; Overbury, S. H.; Sun, S. H.; Dai, S. *Chem. Commun.* **2008**, 4357–4359.
(25) Siswana, N. P.; Trimm, D. L. *Catal. Lett.* **1997**, *46*, 27–29.

exhibit a $T_{1/2}$ of −25 °C, compared to a value of 30 °C for the conventional Au/Fe_2O_3, while the temperature was 67 °C for $Pt-Fe_3O_4$ NPs versus ~100 °C for conventional Pt/Fe_2O_3. The enhanced activities thus unambiguously unveil the superior support effect of metal oxide in the solution-processed noble metal−metal oxide NPs with intrinsic epitaxial particle linkage, which would not only provide stronger electronic interaction and a larger heterojunction interface but also enhance the thermal stability of the noble metal NPs against particle sintering.[24]

Conclusion

This work reported a general synthetic approach to composite noble metal−metal oxide nanoparticles by seed-mediated growth. With presynthesized noble metal seeds, metal oxides were grown over them by thermal decomposition of metal carbonyl followed by oxidation in air. The formed NPs possess a dumbbell-like morphology and were found to contain intrinsic epitaxial linkage between the two components. Such nanoparticles were found to be highly active for catalyzing CO oxidation with a performance superior to that of the similar catalysts prepared by conversional methods. These heterostructured nanoparticles represent a new generation of advanced heterogeneous nanomaterials and could have great potential for catalytic and biological applications.

Acknowledgment. This work was supported by National Science Foundation Grant DMR 0606264 and the Brown University Seed Fund. H.Y. and S.D. were supported by the Division of Chemical Sciences, Geosciences, and Biosciences, Office of Basic Energy Sciences, U.S. Department of Energy.

Supporting Information Available: Experimental details and more material characterizations. This material is available free of charge via the Internet at http://pubs.acs.org.